

## Flow harmonics of charmonium states in heavy ion collisions

---

**Sungtae Cho\***

*Division of Science Education, Kangwon National University, Chuncheon 24341, Korea*

*E-mail: [sungtae.cho@kangwon.ac.kr](mailto:sungtae.cho@kangwon.ac.kr)*

We discuss the flow harmonics or the elliptic and triangular flow of  $J/\psi$ ,  $\psi(2S)$ , and  $\chi_c(1P)$  mesons in heavy ion collisions. Starting from the investigation on transverse momentum distributions of those charmonium states, we calculate their elliptic and triangular flow when they are produced at the quark-hadron phase boundary by quark recombination. We show that the wave function distribution of charmonium states plays a significant role, especially in producing charmonium states, leading to the transverse momentum distribution of the  $\psi(2S)$  meson as large as that of the  $J/\psi$  meson. On the other hand, we find that the wave function effects and feed-down contributions are averaged out for elliptic and triangular flow, resulting in similar elliptic and triangular flow for all charmonium states. We further investigate the elliptic and triangular flow of charmonium states at low transverse momentum regions and discuss the quark number scaling of elliptic and triangular flow for charmonium states in heavy ion collisions.

*10th International Conference on Quarks and Nuclear Physics (QNP2024)  
8-12 July, 2024  
Barcelona, Spain*

---

\*Speaker

## 1. Introduction

Since the  $J/\psi$  meson has been proposed as one of tools for verifying the existence of the quark-gluon plasma (QGP) in heavy ion collisions [1], charmonium states have been considered as important probes to study the various properties of the QGP. With the help of much larger energy at the Large Hadron Collider (LHC), charmonium states are expected to be more produced than before, thereby providing us with more information on many properties of the QGP [2].

The recent measurement by ALICE Collaboration shows that the  $R_{AA}$  of the  $\psi(2S)$  as well as  $J/\psi$  is enhanced at low transverse momentum regions [3], strongly supporting the formation of charmonium states by recombination in the QGP. Nevertheless, the measurement on the  $R_{AA}$  between the  $\psi(2S)$  and  $J/\psi$  shows different behavior [3], implying that the production of the  $J/\psi$  and  $\psi(2S)$  is affected differently when they are formed from the QGP by recombination in heavy ion collisions. Reminding that both  $J/\psi$  and  $\psi(2S)$  mesons share the same source for their constituents, one can consider different amounts of yields for different charmonium states due to different coalescence probabilities, or the different Wigner functions.

The dependence of the charmonia production on their internal structures, or their wave functions when they are produced from the QGP by recombination has already been studied [4], and it has been shown that the  $\psi(2S)$  meson can be more produced than expected by the statistical hadonization model [4]. Along with this observation, we investigate the dependence of charmonia flow on their internal structures based on quark coalescence [5], as the flow also depends on the Wigner function via the transverse momentum distribution of the hadron. It is expected that different transverse momentum distributions give rise to different flows for different charmonium states [6]. In addition, we study the so-called *number of constituent quark scaling of elliptic flows* [7], for the various flow harmonics charmonium states when charmonium states of different structures are formed from the same source of charm quarks by coalescence.

## 2. Transverse momentum distributions of charmonium states

The transverse momentum distribution of charmonium states is given by [4, 6],

$$\frac{d^2N}{dp_T^2} = \frac{g}{V} \int d^3\vec{r} d^2\vec{p}_{cT} d^2\vec{p}_{\bar{c}T} \delta^{(2)}(\vec{p}_T - \vec{p}_{cT} - \vec{p}_{\bar{c}T}) \frac{d^2N_c}{dp_{cT}^2} \frac{d^2N_{\bar{c}}}{dp_{\bar{c}T}^2} W(\vec{r}, \vec{k}), \quad (1)$$

where  $W(\vec{r}, \vec{k})$  is the Wigner function composed of wave functions of charmonia. The factor  $g$  is the degeneracy for each charmonium. As seen in Eq. (1), it largely consists of two parts, the Wigner function and the transverse momentum distribution of charm quarks. Considering that all different charmonium states share the same charm constituents, one finds that it is the Wigner function that plays a key role in making the production of different charmonium states different [4].

Hence, we apply here different Wigner functions for different charmonium states to calculate the transverse momentum distribution for different charmonium states. The Wigner functions based on Gaussian wave functions for  $d$ -wave [8] and  $2S$  [4] states are,

$$\begin{aligned} W_d(\vec{r}, \vec{k}) &= \frac{8}{15} \left( 4 \frac{r^4}{\sigma^4} - 20 \frac{r^2}{\sigma^2} + 15 - 20\sigma^2 k^2 + 4\sigma^4 k^4 + 16r^2 k^2 - 8(\vec{r} \cdot \vec{k})^2 \right) e^{-\frac{r^2}{\sigma^2} - k^2 \sigma^2}, \\ W_{2S}(\vec{r}, \vec{k}) &= \frac{16}{3} \left( \frac{r^4}{\sigma^4} - 2 \frac{r^2}{\sigma^2} + \frac{3}{2} - 2\sigma^2 k^2 + \sigma^4 k^4 - 2r^2 k^2 + 4(\vec{r} \cdot \vec{k})^2 \right) e^{-\frac{r^2}{\sigma^2} - k^2 \sigma^2}, \end{aligned} \quad (2)$$

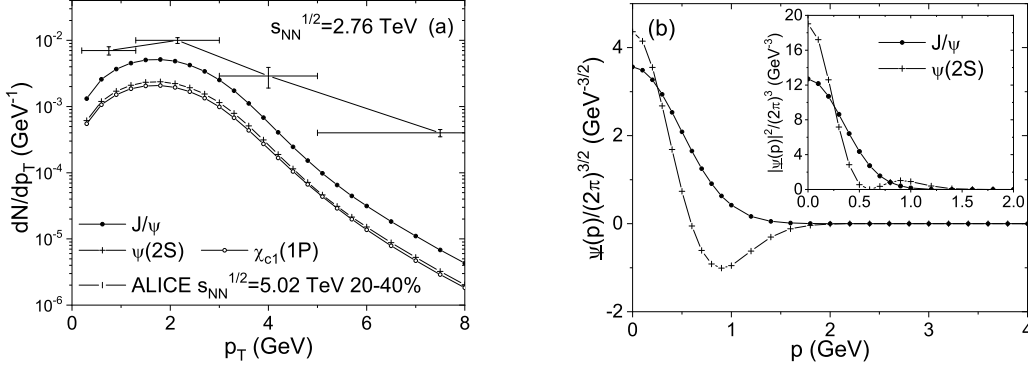


**Figure 1:** (a) Transverse momentum distributions,  $dN/dp_T$  of charmonium states at midrapidity in 0-10 % centrality at LHC,  $\sqrt{s_{NN}} = 2.76$  TeV. Also shown for comparison is the experimental measurement of the  $J/\psi$  measured at LHC,  $\sqrt{s_{NN}} = 5.02$  TeV,  $|y| < 0.9$  in 20-40 % centrality [12]. (b) Gaussian wave function distributions of the  $J/\psi$  and  $\psi(2S)$  divided by  $(2\pi)^{3/2}$  in a momentum space. In the inset of the figure the wave function squares in a momentum space,  $|\tilde{\psi}(p)|^2/(2\pi)^3$  for the  $J/\psi$  and  $\psi(2S)$  are shown.

with an oscillator frequency  $\omega$  being related to  $\sigma$  via  $\sigma^2 = 1/(\mu\omega)$ . One can calculate further Eq. (1) to obtain the transverse momentum distribution of charmonia in a more simplified form,

$$\frac{d^2N}{dp_T^2} = \frac{g_M}{V} \int d^2\vec{p}_{cT} d^2\vec{p}_{\bar{c}T} \delta^{(2)}(\vec{p}_T - \vec{p}_{cT} - \vec{p}_{\bar{c}T}) \frac{d^2N_c}{dp_{cT}^2} \frac{d^2N_{\bar{c}}}{dp_{\bar{c}T}^2} |\tilde{\psi}(\vec{k})|^2. \quad (3)$$

with the help of one of important properties of the Wigner function [9],  $\int d^3\vec{r} W(\vec{r}, \vec{k}) = |\tilde{\psi}(\vec{k})|^2$ . The  $\tilde{\psi}(\vec{k})$  is the wave function in momentum space, transformed from the coordinate space wave function used in the Wigner function,  $\psi(\vec{r})$ .

In order to evaluate Eq. (3) we use an oscillator frequency,  $\omega = 0.076$  GeV at LHC obtained from the requirement that all charm quarks at zero transverse momentum should be hadronized by coalescence [10]. For the transverse momentum distribution of charm quarks, we adopt  $d^2N_c/dp_{cT}^2$  at midrapidity in 0-10% centrality [11], presenting  $dN_c/dy=14.9$  at LHC for the total number of charm quark pairs at a unit midrapidity interval,  $|y| < 0.5$  in the system.

Shown in Fig. 1 (a) is the transverse momentum distributions,  $dN/dp_T$  of charmonium states evaluated at midrapidity in 0-10 % centrality at LHC,  $\sqrt{s_{NN}} = 2.76$  TeV. Also shown for comparison is the experimental measurement of the  $J/\psi$  at LHC,  $\sqrt{s_{NN}} = 5.02$  TeV,  $|y| < 0.9$  in 20-40 % centrality [12]. Here we use the coalescence volume  $3530 \text{ fm}^3$  for LHC, and consider the charm quark mass of 1.5 GeV [10, 13]. We also take into account the contributions from the decay of heavier charmonium states. As shown in Fig. 1 (a), the transverse momentum distribution of the  $\psi(2S)$  is found to be comparable to that of the  $J/\psi$ , reaching as half large as that of the  $J/\psi$  when they are initially produced from charm quarks by recombination. The reason for the enhancement in the production of the  $\psi(2S)$  meson compared to the estimation in the statistical hadronization model turns out to be the large amount of the squared wave function of the  $\psi(2S)$  at low transverse momentum regions, enabling the large overlap with its Wigner function [4] as shown in Fig. 1 (b).

### 3. Elliptic and triangular flow of charmonium states

We now calculate the charmonia flow harmonics, represented as  $v_n$ , the  $n$ -th coefficient in the Fourier expansion of flows [5, 7]

$$v_n(p_T) = \langle \cos(n(\psi - \Psi_n)) \rangle = \frac{\int d\psi \cos(n(\psi - \Psi_n)) \frac{d^2N}{dp_T^2}}{\int d\psi \frac{d^2N}{dp_T^2}}, \quad \Psi_n = \frac{1}{n} \tan^{-1} \left( \frac{\langle p_T \sin(n\psi) \rangle}{\langle p_T \cos(n\psi) \rangle} \right) \quad (4)$$

with  $p_T$  and  $\psi$  being, respectively, the transverse momentum and azimuthal angle of the charmonium in the transverse plane perpendicular to the collision axis. The  $\Psi_n$  is the event-plane angle defined in the region,  $-\pi/n < \Psi_n < \pi/n$ . We adopt here the transverse momentum distributions of the charmonium,  $d^2N/dp_T^2$  obtained in the previous section with a Fourier expansion of the charm quark transverse momentum spectrum, and also the flow harmonics of a charm quark by the POWLANG transport analysis [14]. Accordingly, we consider the event-averaged flow harmonics of charmonium states on averaged events, as the flow harmonics of charm quarks in the POWLANG transport study have also been averaged over events [14],

$$v_n(p_T) = \frac{\frac{n}{2\pi} \int_{-\pi/n}^{\pi/n} \int d\psi \cos(n(\psi - \Psi_n)) \frac{d^2N}{dp_T^2} d\Psi_n}{\frac{n}{2\pi} \int_{-\pi/n}^{\pi/n} \int d\psi \frac{d^2N}{dp_T^2} d\Psi_n} = \frac{v_{nN}(p_T)}{v_{nD}(p_T)}. \quad (5)$$

As shown in Fig. 2, flow harmonics of charmonium states, the  $J/\psi$ ,  $\psi(2S)$  and  $\chi_c(1P)$  meson are almost the same. Even though the transverse momentum distributions are different for each charmonium state, as discussed in the previous section, the elliptic and triangular flow of different charmonium states are found to be almost the same. We find that the reason for almost the same flow harmonics for the above charmonium states is attributable to the characteristics of the  $v_n$  itself; defined as the average value of cosine in different orders  $n$  over transverse momenta.

We show in Fig. 2 (c) and (d) the numerator  $v_{2N}(p_T)$  and denominator  $v_{2D}(p_T)$  parts of the charmonia elliptic flow in Eq. (5) at the same LHC energy in the same POWLANG transport setup. One finds the explicit dependence of both the numerator and denominator part of  $v_n$  on different charmonium states. The similar amounts of contribution from different transverse momentum distributions of charmonium states to both the numerator and denominator of the  $v_n$  are cancelled out of each other, giving rise to almost the same flow harmonics for all charmonium states.

Shown in Fig. 2 (e) and (f) are re-scaled elliptic and triangular flows of charmonium states,  $v_n(p_T/2)/2$  calculated from those in Fig. 2 (a) and (b), respectively. Also shown are the corresponding flow harmonics of charm quarks  $v_{2,c}(p_T)$  (e) or  $v_{3,c}(p_T)$  (f) for comparison. We find that the elliptic flow of charmonium states satisfy the relation, *the number of constituent quark scaling of elliptic flows*,  $v_{2,c\bar{c}}(p_T) \approx 2v_{2,c}(p_T/2)$  as shown in Fig. 2 (e). Similarly, we also see that the above relation holds for the triangular flow of charmonium states,  $v_{3,c\bar{c}}(p_T) \approx 2v_{3,c}(p_T/2)$  as shown in Fig. 2 (f).

### 4. Conclusions

We have discussed here the second and third flow harmonics of charmonium states in heavy ion collisions. Starting from the investigation on Wigner functions for  $J/\psi$ ,  $\psi(2S)$ , and  $\chi_c(1P)$

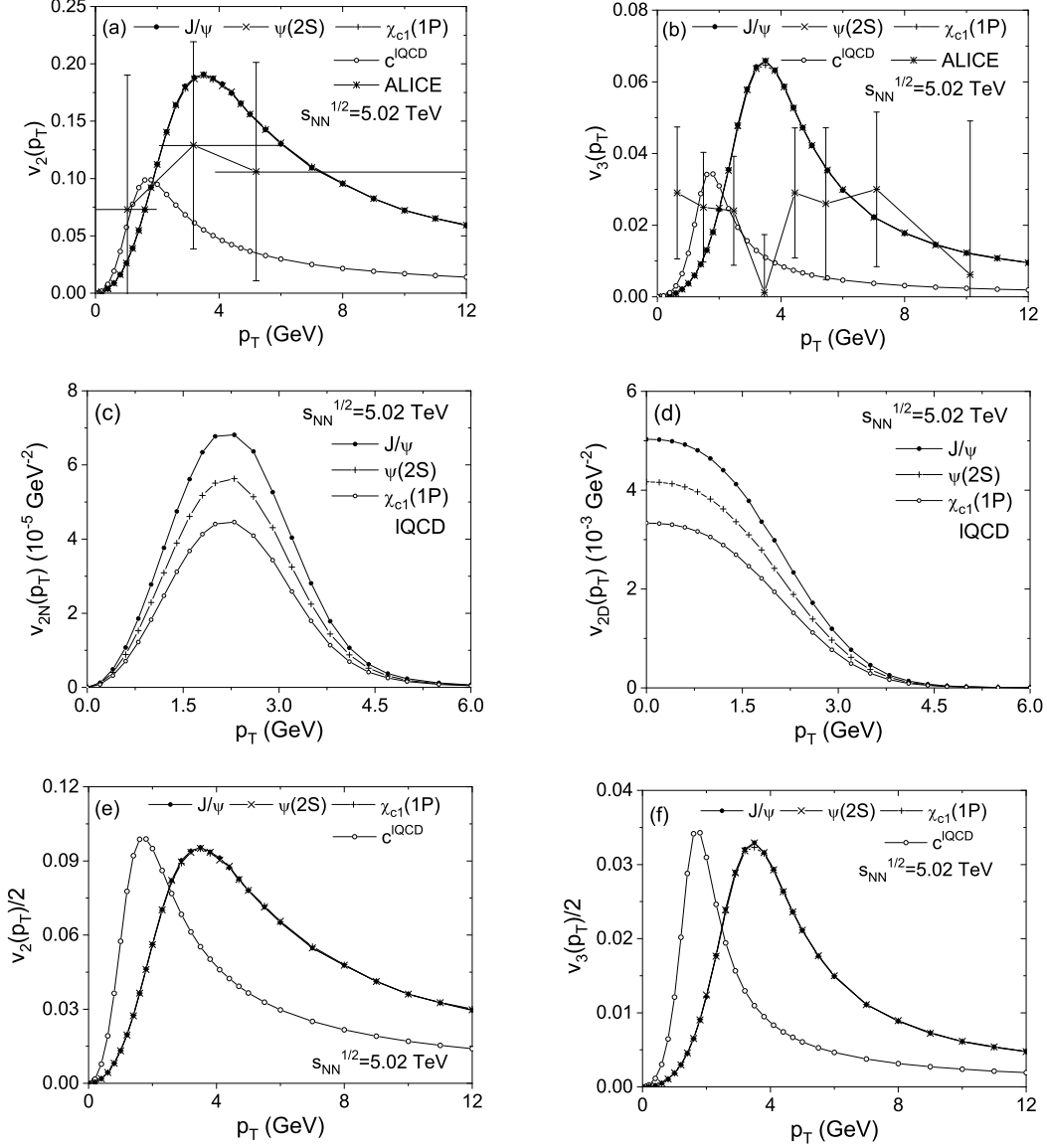


**Figure 2:** Elliptic (a) and triangular flow (b) of charmonium states calculated from those of charm quarks based on the IQCD transport coefficients in the POWLANG transport at LHC,  $\sqrt{s_{NN}}=5.02$  TeV, together with the measurement of the  $J/\psi$  elliptic flow (a) in rapidity  $|y| < 0.9$  in 20-40 % centrality [15] and the  $J/\psi$  triangular flow (b) in rapidity range of  $2.5 < y < 4.0$  in 30-50% centrality [16]. Also shown is the corresponding flow harmonics of bare charm quarks in each figure for comparison. We also show the numerator (c) and denominator (d) parts of the charmonia elliptic flow in Eq. (5) at the same LHC energy in the same POWLANG transport setup [14], denoted by  $v_{2N}(p_T)$  (c) and  $v_{2D}(p_T)$  (d), respectively. Lastly, we show re-scaled elliptic and triangular flow of charmonium states,  $v_2(p_T)/2$  (e) and  $v_3(p_T)/2$  (f) calculated from those in Fig. 2 (a) and (b), respectively. We also show the corresponding flow harmonics of bare charm quarks,  $v_{2,c}(p_T)$  (e) and  $v_{3,c}(p_T)$  (f) for comparison.

mesons we have evaluated the transverse momentum distributions for those charmonium states. We have observed the explicit dependence of transverse momentum distributions of charmonium states on their internal structures through their wave functions.

We then have considered charmonia flow harmonics, or  $v_2$  and  $v_3$  to study also the possible dependence of the flow of charmonium states on their internal structures via their transverse momentum distributions. We have found that the elliptic and triangular flow of  $J/\psi$ ,  $\psi(2S)$  and  $\chi_c(1P)$  mesons are only slightly different, though both the numerator and denominator part of  $v_n$  are actually dependent on their internal structures. We have also studied the relation between the flow of charmonium states and their constituent quarks for charmonium states, and have found that the relation holds very well for charmonium states,  $v_{n,c\bar{c}}(p_T) \approx 2v_{n,c}(p_T/2)$  with both  $n = 2$  and  $3$ .

We consider that investigating charmonia production presents us with one of the valuable chances to understand the production of hadrons formed from both the same number and kind of constituents with different internal structures. Therefore, studying not only the transverse momentum distributions and anisotropic flow, but also other closely relevant observables of the charmonium states would help us to understand in more detail the hadron production mechanism in heavy ion collisions, broadening our understanding on the properties of the quark-gluon plasma.

## References

- [1] T. Matsui and H. Satz, *Phys. Lett. B* **178**, 416 (1986).
- [2] R. L. Thews, M. Schroedter and J. Rafelski, *Phys. Rev. C* **63**, 054905 (2001).
- [3] S. Acharya *et al.* (ALICE Collaboration), *Phys. Rev. Lett.* **132**, no.4, 042301 (2024).
- [4] S. Cho, *Phys. Rev. C* **91**, no. 5, 054914 (2015).
- [5] V. Greco, C. M. Ko, and P. Levai, *Phys. Rev. C* **68**, 034904 (2003).
- [6] S. Cho, *Phys. Rev. C* **109**, no.5, 054904 (2024).
- [7] D. Molnar and S. A. Voloshin, *Phys. Rev. Lett.* **91**, 092301 (2003).
- [8] S. Cho *et al.* (ExHIC Collaboration), *Phys. Rev. C* **84**, 064910 (2011).
- [9] M. Hillery, R. F. O'Connell, M. O. Scully and E. P. Wigner, *Phys. Rept.* **106**, 121 (1984).
- [10] S. Cho and S. H. Lee, *Phys. Rev. C* **101**, no. 2, 024902 (2020).
- [11] S. Plumari *et al.*, *Eur. Phys. J. C* **78**, no. 4, 348 (2018).
- [12] S. Acharya *et al.* (ALICE Collaboration), *Phys. Lett. B* **805**, 135434 (2020).
- [13] S. Cho *et al.* (ExHIC Collaboration), *Prog. Part. Nucl. Phys.* **95**, 279 (2017).
- [14] A. Beraudo, A. De Pace, M. Monteno, M. Nardi and F. Prino, *JHEP* **02**, 043 (2018).
- [15] S. Acharya *et al.* (ALICE Collaboration), *Phys. Rev. Lett.* **119**, no. 24, 242301 (2017).
- [16] S. Acharya *et al.* (ALICE Collaboration), *JHEP* **2010**, 141 (2020).